

1 Supplement of

2 **Comprehensive characterization of the particulate IVOCs and**
3 **SVOCs from heavy-duty diesel vehicles using two-dimensional**
4 **gas chromatography time-of-flight mass spectrometry**

5 Xiao He¹, Xuan Zheng^{1*}, Shaojun Zhang^{2,3}, Xuan Wang⁴, Ting Chen¹, Xiao Zhang², Guanghan Huang², Yihuan
6 Cao², Liqiang He², Xubing Cao⁵, Yuan Cheng⁵, Shuxiao Wang^{2,3}, Ye Wu^{2,6*}

7 ¹College of Chemistry and Environmental Engineering, Shenzhen University, Shenzhen 518060, China

8 ²School of Environment, State Key Joint Laboratory of Environment Simulation and Pollution Control, Tsinghua University,
9 Beijing 100084, China

10 ³State Environmental Protection Key Laboratory of Sources and Control of Air Pollution Complex, Beijing 100084, China

11 ⁴School of Energy and Environment, City University of Hong Kong, Hong Kong SAR, China

12 ⁵State Key Laboratory of Urban Water Resource and Environment, School of Environment, Harbin Institute of Technology,
13 Harbin, 150090, China

14 ⁶Beijing Laboratory of Environmental Frontiers Technologies, Beijing 100084, China

15 *Correspondence to:* Xuan Zheng (x-zheng11@szu.edu.cn), Ye Wu (ywu@mail.tsinghua.edu.cn)

16 **Text S1. Authentic standards, internal standards, and instrumental analysis**

17 The authentic standards include 25 *n*-alkanes (C₁₃-C₃₇), 6 *n*-alkenes (C₁₀, C₁₂, C₁₄, C₁₆, C₁₈, C₂₀),
18 isophorone, 2 benzylic ketone esters, 2 cycloalkanes, 2-5 ring PAHs, 4 phenol benzylic alcohols, and 5
19 Nitros. The list of authentic standards is presented in Table S1

20 The internal standards used in this work include deuterated alkanes (C₁₂D₂₆, C₁₆D₃₄, C₂₀D₄₂, C₂₄D₅₀,
21 C₂₈D₅₈, C₃₂D₆₆), deuterated PAHs (naphthalene-d₈, acenaphthene-d₁₀, phenanthrene-d₁₀, fluoranthene-
22 d₁₀, chrylene-d₁₂, perylene-d₁₂, benzo(a)pyrene-d₁₂), cyclohexane-d₁₂, biphenyl-d₁₀, 1,3,5-
23 trimethylbenzene-d₁₂, and *p*-xylene-d₁₀.

24 **Text S2. Dynamic sampling of field blanks and the quality control/quality assurance**

25 Field blank samples of background dilution air were collected simultaneously on each sampling day to
26 correct for the blank matrix. Filtered ambient air was drawn into the constant volume sampler (CVS,
27 MEXA-7200DTR) and deposited on quartz filter. To maintain consistency, blank sampling duration
28 was 1800 s.

29 In previous studies, two common experimental settings are deployed to characterize the gas-particle (g-
30 p) partitioning of vehicle emitted intermediate-volatility and semi-volatile organic compound
31 (I/SVOCs). The first design places Tenax TA sampling tubes after quartz filters and particulate and
32 gaseous I/SVOCs are collected separately (Zhao et al., 2015). The second design uses bare quartz filter
33 (bare-Q) to collect total I/SVOC compounds and quartz filter behind Teflon filter (QBT) to collect
34 gaseous I/SVOC compounds (May et al., 2013a, 2013b). The adsorption of gaseous I/SVOCs onto
35 filters can cause negative biases in the measured gas phase concentrations and positive artifacts in the
36 measured particle phase concentrations. In the former experimental design, the particulate I/SVOCs are
37 positively biased due to the vapor loss to the quartz filters, whereas in the latter one, total I/SVOCs are
38 negatively biased due to the insufficient collection of gaseous I/SVOCs by quartz filters. Comparing
39 with quartz filters, which absorb vapours significantly (May et al., 2013b). Teflon has small surface
40 area and is relatively inert. Considering the reasons stated above, a Teflon filter is deployed instead of
41 a quartz filter before Tenax TA sampling tubes.

42 **Text S3. The calibration and method detection limit for each authentic standard**

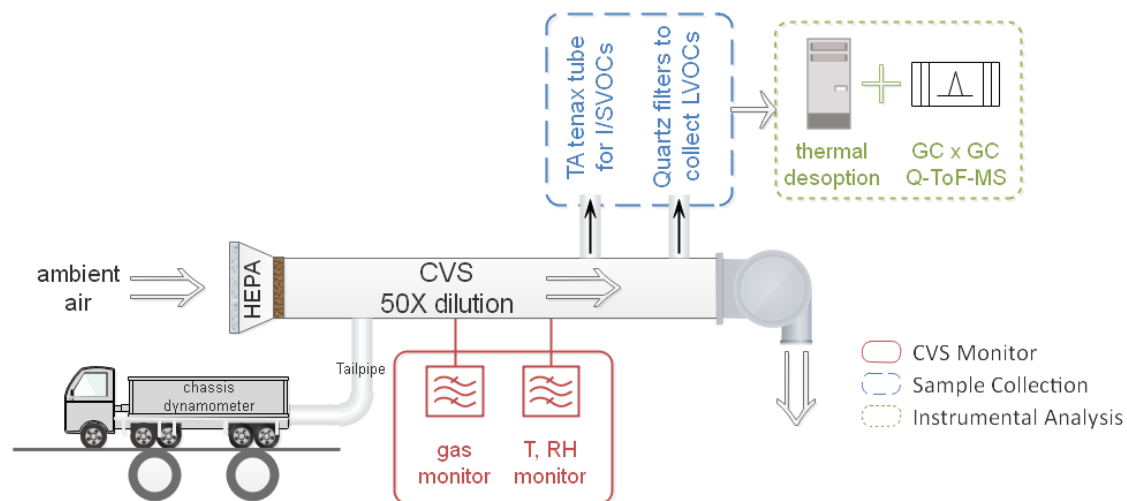
43 The calibration curve for each authentic standard is built by spiking gradient volumes (0, 1, 2, 5, 7, 10
44 μ L) of working solution plus 2 μ L of internal standard solution and establishing a liner relationship
45 between the peak area (PA) ratio (PA of each authentic standard/PA of the corresponding internal
46 standard) and the spiked mass. The method detection limit (MDL) for each authentic standard is
47 determined as half of the minimum mass on the calibration curve and is summarized in Table S1.

48 **Text S4. Calculation of the saturation mass concentration**

49 Saturation mass concentration (C_i^*) of individual n -alkane is calculated using the following equation:

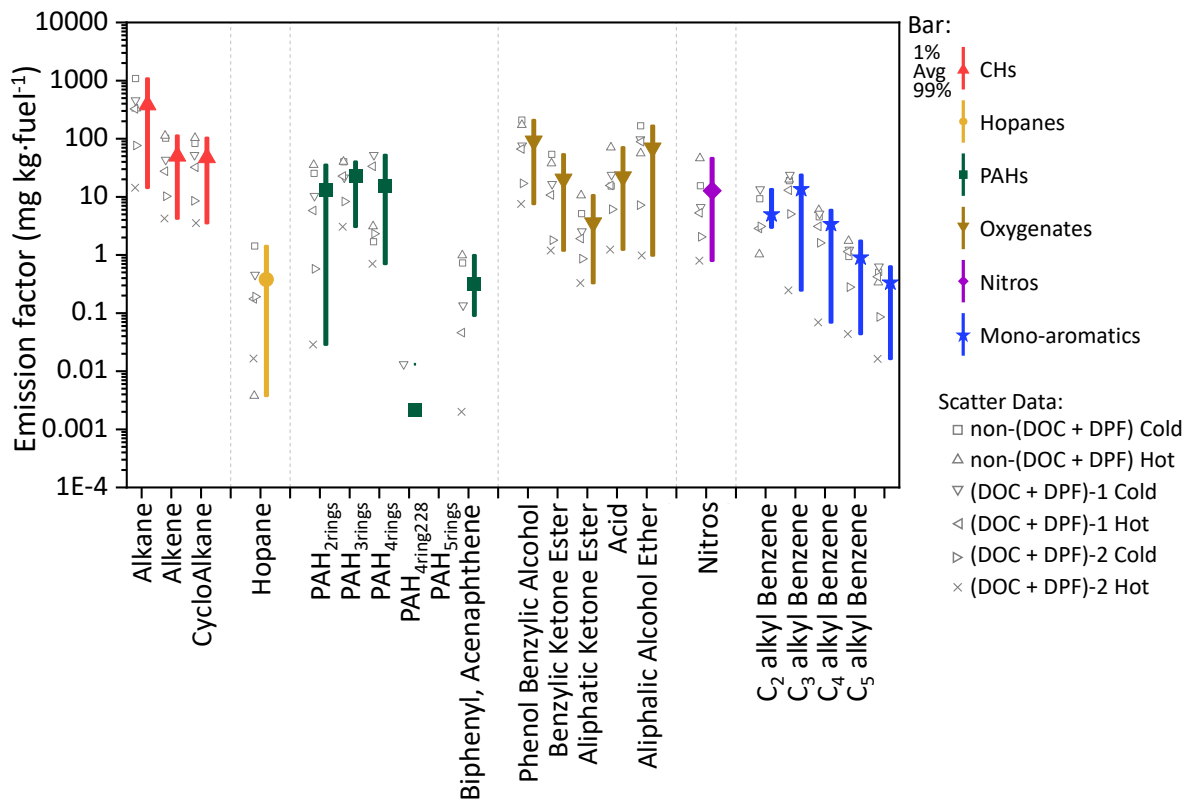
50
$$C_i^* = \frac{M_i 10^6 \zeta_i P_{L,i}^0}{760RT}$$

51 where M_i is the molecular weight of species i (g mol^{-1}); ζ_i is the activity coefficient of species i in the
52 condensed phase and is assumed to be 1; $P_{L,i}^0$ is the liquid vapor pressure (torr) for species i , which is
53 obtained from the US EPA Suite data ([https://www.epa.gov/tsca-screening-tools/download-epi-
54 suitetm-estimation-program-interface-v411](https://www.epa.gov/tsca-screening-tools/download-epi-suitetm-estimation-program-interface-v411)). R is the ideal gas constant ($8.2 \times 10^{-5} \text{ m}^3 \text{ atm mol}^{-1} \text{ K}^{-1}$);
55 T is the air temperature (K).



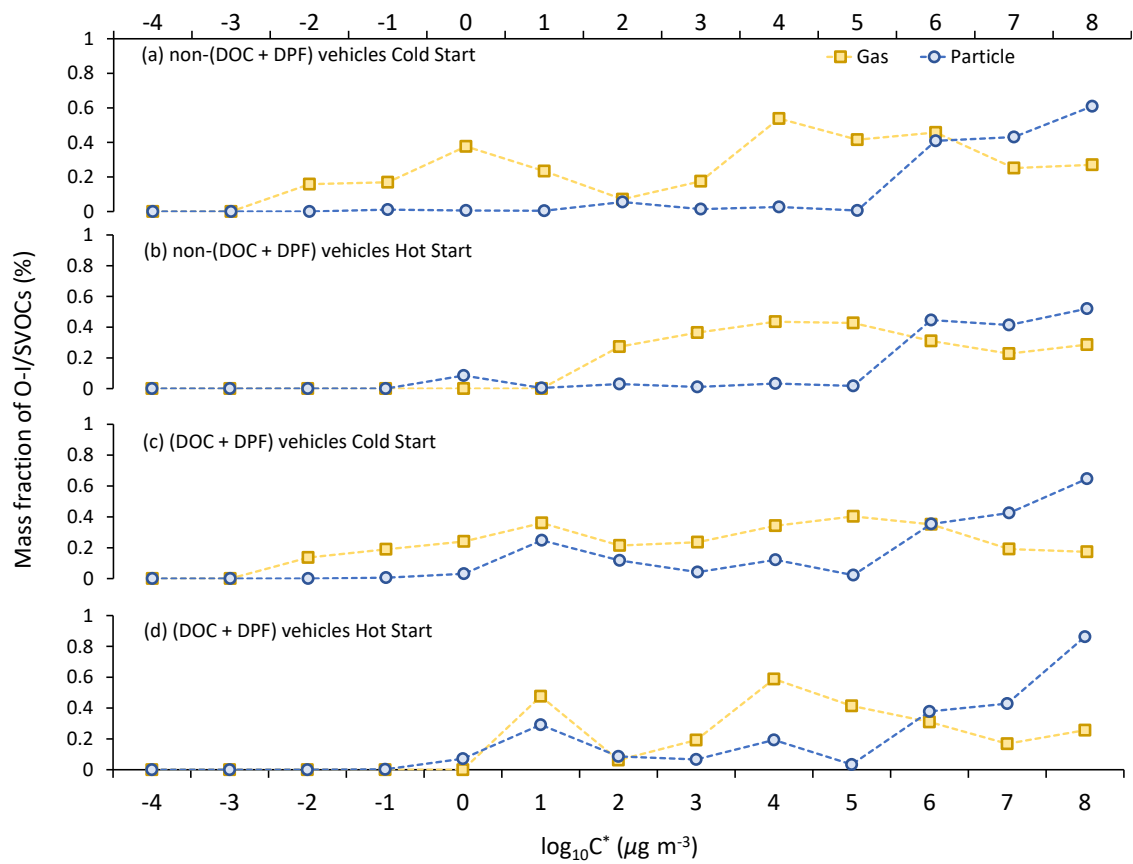
56

57 **Figure S1. Experiment diagram to collect and characterize vehicle emissions. The constant volume sampler (CVS)**
 58 **system, sample collection, and instrumental analysis are highlighted by different colours. The exhaust is drawn into**
 59 **the CVS system, from which multiple sampling trains are assembled for different analysis purposes.**



60
61
62
63
64

Figure S2. The measured emission factor (mg kg-fuel^{-1}) of the twenty-one categories of the HDDV-emitted I/SVOCs in the gas phase. Coloured-bars and coloured-scatters/shaped-scatters represent different organic species and driving cycles. The square dots in the middle of each bar denote the average value and the lower and upper boundaries of the bar denote the 1% and 99% percentile of the values.



65
66

Figure S3. Mass fraction of O-I/SVOCs in the gas and particle phases in each volatility bins.

67 Table S1. List of the authentic standards, corresponding internal standards, and the method detection limit (MDL).

| Name | Formula | Internal Standard | 1 st RT (s) | 2 nd RT (s) | MDL (μg) |
|------------------------------------|---|---------------------------------------|------------------------|------------------------|-----------------------|
| <i>n</i> -Alkane | | | | | |
| Tridecane | C ₁₃ H ₂₈ | <i>n</i> -Dodecane-d ₂₆ | 1208 | 0.93 | 0.0005 |
| Tetradecane | C ₁₄ H ₃₀ | <i>n</i> -Hexadecane-d ₃₄ | 1368 | 0.94 | 0.0005 |
| Pentadecane | C ₁₅ H ₃₂ | <i>n</i> -Hexadecane-d ₃₄ | 1520 | 0.96 | 0.0005 |
| Hexadecane | C ₁₆ H ₃₄ | <i>n</i> -Hexadecane-d ₃₄ | 1660 | 0.97 | 0.0005 |
| Heptadecane | C ₁₇ H ₃₆ | <i>n</i> -Hexadecane-d ₃₄ | 1796 | 0.99 | 0.0005 |
| Octadecane | C ₁₈ H ₃₈ | <i>n</i> -Eicosane-d ₄₂ | 1924 | 1 | 0.0005 |
| Nonadecane | C ₁₉ H ₄₀ | <i>n</i> -Eicosane-d ₄₂ | 2044 | 1.02 | 0.0005 |
| Eicosane | C ₂₀ H ₄₂ | <i>n</i> -Eicosane-d ₄₂ | 2160 | 1.03 | 0.0005 |
| Heneicosane | C ₂₁ H ₄₄ | <i>n</i> -Eicosane-d ₄₂ | 2272 | 1.05 | 0.0005 |
| Docosane | C ₂₂ H ₄₆ | <i>n</i> -Tetracosane-d ₅₀ | 2376 | 1.06 | 0.0005 |
| <i>n</i> -Tricosane | C ₂₃ H ₄₈ | <i>n</i> -Tetracosane-d ₅₀ | 2480 | 1.08 | 0.0005 |
| Tetracosane | C ₂₄ H ₅₀ | <i>n</i> -Tetracosane-d ₅₀ | 2576 | 1.09 | 0.0005 |
| Pentacosane | C ₂₅ H ₅₂ | <i>n</i> -Tetracosane-d ₅₀ | 2672 | 1.11 | 0.0005 |
| Hexacosane | C ₂₆ H ₅₄ | <i>n</i> -Octacosane-d ₅₈ | 2760 | 1.13 | 0.0005 |
| Heptacosane | C ₂₇ H ₅₆ | <i>n</i> -Octacosane-d ₅₈ | 2848 | 1.15 | 0.0005 |
| Octacosane | C ₂₈ H ₅₈ | <i>n</i> -Octacosane-d ₅₈ | 2932 | 1.17 | 0.0005 |
| <i>n</i> -Nonacosane | C ₂₉ H ₆₀ | <i>n</i> -Octacosane-d ₅₈ | 3016 | 1.19 | 0.0005 |
| <i>n</i> -Triacontane | C ₃₀ H ₆₂ | <i>n</i> -Octacosane-d ₅₈ | 3092 | 1.23 | 0.0005 |
| <i>n</i> -Hentriacontane | C ₃₁ H ₆₄ | <i>n</i> -Octacosane-d ₅₈ | 3168 | 1.26 | 0.0005 |
| <i>n</i> -Dotriacontane | C ₃₂ H ₆₆ | <i>n</i> -Octacosane-d ₅₈ | 3244 | 1.3 | 0.0005 |
| <i>n</i> -Tritriacontane | C ₃₃ H ₆₈ | <i>n</i> -Octacosane-d ₅₈ | 3316 | 1.41 | 0.0005 |
| <i>n</i> -Tetraatriacontane | C ₃₄ H ₇₀ | <i>n</i> -Octacosane-d ₅₈ | 3456 | 1.9 | 0.0005 |
| <i>n</i> -Pentatriacontane | C ₃₅ H ₇₂ | <i>n</i> -Octacosane-d ₅₈ | 3556 | 2.2 | 0.0005 |
| <i>n</i> -Hexatriacontane | C ₃₆ H ₇₄ | <i>n</i> -Octacosane-d ₅₈ | 3676 | 2.58 | 0.0005 |
| <i>n</i> -Heptatriacontane | C ₃₇ H ₇₆ | <i>n</i> -Octacosane-d ₅₈ | 3820 | 3.02 | 0.0005 |
| <i>n</i> -Alkene | | | | | |
| 1-Tetradecene | C ₁₄ H ₂₈ | <i>n</i> -Dodecane-d ₂₆ | 1356 | 0.99 | 0.00019 |
| 1-Cetene | C ₁₆ H ₃₂ | <i>n</i> -Hexadecane-d ₃₄ | 1652 | 1.01 | 0.00019 |
| 1-Octadecene | C ₁₈ H ₃₆ | <i>n</i> -Hexadecane-d ₃₄ | 1916 | 1.04 | 0.00018 |
| 1-Eicosene | C ₂₀ H ₄₀ | <i>n</i> -Eicosane-d ₄₂ | 2152 | 1.07 | 0.00019 |
| 1-Docosene | C ₂₂ H ₄₄ | <i>n</i> -Eicosane-d ₄₂ | 2420 | 1.22 | 0.00019 |
| Benzylic Ketone Ester | | | | | |
| Dimethyl phthalate | C ₁₀ H ₁₀ O | Phenanthrene-d ₁₀ | 1512 | 2.58 | 0.0005 |
| Diethyl Phthalate | C ₁₂ H ₁₄ O | Phenanthrene-d ₁₀ | 1712 | 2.38 | 0.0005 |
| Cycloalkane | | | | | |
| Cyclohexane, octyl- | C ₁₄ H ₂₈ | <i>n</i> -Dodecane-d ₂₆ | 1440 | 1.08 | 0.00018 |
| Cyclohexane, decyl- | C ₁₆ H ₃₂ | <i>n</i> -Hexadecane-d ₃₄ | 1736 | 1.12 | 0.00018 |
| PAH ₂ rings | | | | | |
| Naphthalene, 1-methyl- | C ₁₁ H ₁₀ | Naphthalene-d ₈ | 1200 | 1.97 | 0.0005 |
| Naphthalene, 2-methyl- | C ₁₁ H ₁₀ | Naphthalene-d ₈ | 1228 | 2.04 | 0.0005 |
| Naphthalene, 2-ethyl- | C ₁₂ H ₁₂ | Naphthalene-d ₈ | 1368 | 1.99 | 0.0001 |
| PAH ₃ rings | | | | | |
| Acenaphthene | C ₁₂ H ₁₀ | Acenaphthene-d ₁₀ | 1444 | 2.37 | 0.0005 |
| Acenaphthylene | C ₁₂ H ₈ | Acenaphthene-d ₁₀ | 1500 | 2.27 | 0.0005 |
| Fluorene | C ₁₃ H ₁₀ | Acenaphthene-d ₁₀ | 1640 | 2.32 | 0.0005 |
| Phenanthrene | C ₁₄ H ₁₀ | Phenanthrene-d ₁₀ | 1904 | 2.66 | 0.0005 |
| Anthracene | C ₁₄ H ₁₀ | Phenanthrene-d ₁₀ | 1916 | 2.65 | 0.0005 |
| PAH ₄ rings | | | | | |
| Fluoranthene | C ₁₆ H ₁₀ | Chrysene-d ₁₂ | 2236 | 2.93 | 0.0005 |
| Pyrene | C ₁₆ H ₁₀ | Chrysene-d ₁₂ | 2292 | 3.14 | 0.0005 |
| Benz[a]anthracene | C ₁₈ H ₁₂ | Chrysene-d ₁₂ | 2640 | 3.31 | 0.0005 |
| Chrysene | C ₁₈ H ₁₂ | Chrysene-d ₁₂ | 2648 | 3.42 | 0.0005 |
| PAH ₅ rings | | | | | |
| Benzo[a]pyrene | C ₂₀ H ₁₂ | Chrysene-d ₁₂ | 3012 | 0 | 0.0005 |
| Phenol Benzylic Alcohol | | | | | |
| Phenol | C ₆ H ₆ O | Phenanthrene-d ₁₀ | 680 | 1.89 | 0.0005 |
| Phenol, 2-methyl- | C ₇ H ₈ O | Phenanthrene-d ₁₀ | 824 | 1.92 | 0.0005 |
| <i>p</i> -Cresol | C ₇ H ₈ O | Phenanthrene-d ₁₀ | 864 | 1.92 | 0.0005 |
| Phenol, 2,4-dimethyl- | C ₈ H ₁₀ O | Phenanthrene-d ₁₀ | 1004 | 1.91 | 0.0005 |
| Nitros | | | | | |
| 1-Propanamine, N-nitroso-N-propyl- | C ₆ H ₁₄ N ₂ O | Phenanthrene-d ₁₀ | 860 | 1.91 | 0.0005 |
| Benzene, nitro- | C ₆ H ₅ NO ₂ | Phenanthrene-d ₁₀ | 888 | 2.36 | 0.0005 |

| | | | | | |
|--------------------------------|---|------------------------------|------|------|--------|
| <i>o</i> -Nitroaniline | C ₆ H ₆ N ₂ O ₂ | Phenanthrene-d ₁₀ | 1444 | 2.96 | 0.0005 |
| Benzene, 2-methyl-1,3-dinitro- | C ₇ H ₆ N ₂ O ₄ | Phenanthrene-d ₁₀ | 1524 | 2.88 | 0.0005 |
| Benzene, 1-methyl-2,4-dinitro- | C ₇ H ₆ N ₂ O ₄ | Phenanthrene-d ₁₀ | 1632 | 2.81 | 0.0005 |
| Azobenzene | C ₁₂ H ₁₀ N ₂ | Phenanthrene-d ₁₀ | 1756 | 2.4 | 0.0005 |

68

69
70**Table S2. A category-by-category EFs of I/SVOCs in the gas and particle phases for the non-(DOC + DPF) vehicles (Avg_{w0AT}) and (DOC + DPF) vehicles (Avg_{wiAT}) and the removal efficiency.**

| | Particle | | | | Gas | | | |
|------------------------------|------------------------|-------------------------|-------------------------|-----------------------|--------------------|-------------------------|-------------------------|-----------------------|
| | Avg _a II | Avg _{wiA} T | Avg _{w0A} T | Removal Efficiency | Avg _{all} | Avg _{wiA} T | Avg _{w0A} T | Removal Efficiency |
| Alkane | 15.7 0 | 0.25 | 46.60 | 0.99 | 381.6 8 | 218.64 | 707.75 | 0.69 |
| Alkene | 0.44 | 0.05 | 1.22 | 0.96 | 50.02 | 21.37 | 107.33 | 0.80 |
| CycloAlkane | 0.32 | 0.00 | 0.94 | 1.00 | 47.02 | 24.12 | 92.82 | 0.74 |
| Hopane | 0.21 | 0.00 | 0.62 | 1.00 | | | | |
| PAH ₂ rings | 5.78 | 0.13 | 17.06 | 0.99 | 12.91 | 4.19 | 30.35 | 0.86 |
| PAH ₃ rings | 0.66 | 0.07 | 1.85 | 0.96 | 22.62 | 13.89 | 40.07 | 0.65 |
| PAH ₄ rings | 0.22 | 0.00 | 0.65 | 1.00 | 15.60 | 22.20 | 2.40 | -8.25 |
| PAH ₅ rings | 0.13 | 0.00 | 0.40 | 1.00 | | | | |
| Biphenyl, Acenaphthene | 0.01 | 0.00 | 0.02 | 1.00 | 0.32 | 0.05 | 0.86 | 0.95 |
| Phenol Benzylic Alcohol | 1.05 | 0.15 | 2.83 | 0.95 | 91.42 | 41.79 | 190.70 | 0.78 |
| Benzylic Ketone Ester | 0.14 | 0.02 | 0.37 | 0.95 | 20.30 | 7.59 | 45.72 | 0.83 |
| Acid | 0.07 | 0.01 | 0.17 | 0.93 | 3.57 | 1.41 | 7.89 | 0.82 |
| Aliphatic Ketone Ester | 0.30 | 0.04 | 0.81 | 0.95 | 22.14 | 11.71 | 43.01 | 0.73 |
| Aliphatic Alcohol Ether | | | | | 69.45 | 48.60 | 111.16 | 0.56 |
| C ₂ alkyl Benzene | | | | | 4.96 | 4.87 | 5.14 | 0.05 |
| C ₃ alkyl Benzene | | | | | 13.51 | 10.54 | 19.43 | 0.46 |
| C ₄ alkyl Benzene | | | | | 3.39 | 2.47 | 5.22 | 0.53 |
| C ₅ alkyl Benzene | | | | | 0.90 | 0.67 | 1.35 | 0.50 |
| C ₆ alkyl Benzene | | | | | 0.33 | 0.29 | 0.42 | 0.31 |
| Nitros | 0.40 | 0.05 | 1.08 | 0.95 | | | | |
| Total | 25.0 1 | 0.73 | 73.57 | 0.99 | 772.9 4 | 438.14 | 1442.5 4 | 0.70 |

71

72 **Table S3. The distribution of particulate I/SVOCs (mg km⁻¹) at low-speed stage for non-(DPF + DOC) vehicles**
 73 **separated by volatility bins and the O:C ratio.**

| log ₁₀ C * (μg m ⁻³) | O:C ratio | | | | | | | | | | | |
|---|------------|-------------|-------------|-------------|-------------|-------------|-------------|-------------|-------------|-------------|-------------|-------------|
| | 0-0.1 | 0.1- 0.2 | 0.2- 0.3 | 0.3- 0.4 | 0.4- 0.5 | 0.5- 0.6 | 0.6- 0.7 | 0.7- 0.8 | 0.8- 0.9 | 0.9- 1.0 | 1.0- 1.1 | 1.1- 1.2 |
| -4 | 4340. 8 | 2033. 1 | 2210. 9 | 775.5 | 343.8 | 251.6 | 131.3 | 62.0 | 5.4 | 0.0 | 115.0 | 11.0 |
| -3 | 5817. 2 | 3185. 1 | 2259. 7 | 1283. 1 | 467.0 | 320.5 | 240.2 | 77.9 | 41.3 | 0.0 | 35.4 | 21.9 |
| -2 | 664.1 | 321.4 | 268.0 | 129.8 | 54.9 | 41.8 | 26.1 | 9.6 | 9.4 | 0.0 | 7.4 | 0.0 |
| -1 | 226.1 | 38.3 | 46.6 | 16.3 | 13.4 | 11.0 | 1.2 | 2.9 | 0.0 | 0.0 | 0.0 | 1.1 |
| 0 | 66.2 | 17.1 | 0.7 | 0.6 | 0.0 | 0.4 | 0.9 | 0.0 | 0.0 | 0.0 | 25.8 | 0.0 |
| 1 | 398.1 | 19.6 | 5.2 | 1.8 | 0.3 | 0.2 | 0.0 | 1.4 | 0.0 | 0.0 | 23.1 | 0.1 |
| 2 | 173.0 | 29.0 | 94.9 | 0.2 | 0.0 | 0.0 | 1.1 | 2.5 | 0.0 | 0.0 | 0.0 | 0.0 |
| 3 | 296.4 | 107.6 | 3.7 | 4.2 | 0.8 | 3.5 | 0.0 | 0.0 | 0.0 | 0.0 | 0.0 | 0.0 |
| 4 | 108.6 | 12.7 | 43.6 | 26.7 | 2.1 | 0.0 | 0.0 | 0.0 | 0.0 | 0.0 | 0.0 | 0.0 |
| 5 | 47.3 | 22.8 | 83.5 | 87.2 | 28.3 | 201.4 | 14.6 | 3.0 | 0.0 | 0.0 | 0.0 | 0.0 |
| 6 | 460.3 | 197.1 | 116.3 | 30.9 | 29.0 | 15.2 | 0.0 | 0.0 | 0.0 | 0.0 | 0.0 | 0.0 |
| 7 | 887.8 | 715.4 | 215.8 | 200.8 | 39.0 | 163.4 | 0.0 | 0.0 | 0.0 | 0.0 | 0.0 | 0.0 |
| 8 | 89.4 | 158.2 | 11.3 | 7.7 | 32.3 | 44.7 | 36.0 | 12.6 | 0.0 | 0.0 | 6.9 | 0.0 |
| 9 | 806.7 | 49.7 | 4.2 | 103.4 | 13.7 | 259.4 | 45.1 | 0.0 | 0.0 | 0.0 | 17.3 | 0.0 |

74

75 **Table S4. The distribution of particulate I/SVOCs (mg km^{-1}) at middle-speed stage for non-(DPF + DOC) vehicles**
 76 **separated by volatility bins and the O:C ratio.**

| $\log_{10}C$ * ($\mu\text{g m}^{-3}$) | O:C ratio | | | | | | | | | | | |
|--|-----------|---------|---------|---------|---------|---------|---------|---------|---------|---------|---------|---------|
| | 0-0.1 | 0.1-0.2 | 0.2-0.3 | 0.3-0.4 | 0.4-0.5 | 0.5-0.6 | 0.6-0.7 | 0.7-0.8 | 0.8-0.9 | 0.9-1.0 | 1.0-1.1 | 1.1-1.2 |
| -4 | 0.1 | 0.0 | 0.0 | 0.0 | 0.0 | 0.0 | 0.0 | 0.0 | 0.0 | 0.0 | 0.0 | 0.0 |
| -3 | 0.0 | 0.1 | 0.0 | 0.0 | 0.0 | 0.1 | 0.1 | 0.0 | 0.0 | 0.0 | 0.0 | 0.0 |
| -2 | 0.1 | 0.0 | 0.1 | 0.0 | 0.0 | 0.0 | 0.0 | 0.0 | 0.0 | 0.0 | 0.0 | 0.0 |
| -1 | 0.3 | 0.6 | 0.0 | 0.0 | 0.0 | 0.0 | 0.0 | 0.0 | 0.0 | 0.0 | 0.0 | 0.0 |
| 0 | 4.6 | 0.6 | 0.4 | 0.0 | 0.0 | 0.0 | 0.0 | 0.0 | 0.0 | 0.0 | 0.0 | 0.0 |
| 1 | 9.2 | 0.3 | 1.5 | 0.2 | 0.0 | 0.0 | 0.0 | 0.0 | 0.0 | 0.0 | 0.0 | 0.0 |
| 2 | 23.8 | 3.9 | 4.7 | 0.4 | 0.0 | 0.0 | 0.0 | 0.0 | 0.0 | 0.0 | 0.0 | 0.0 |
| 3 | 109. 8 | 11.0 | 1.6 | 0.7 | 0.1 | 0.0 | 0.0 | 0.0 | 0.0 | 0.0 | 0.0 | 0.0 |
| 4 | 172. 4 | 5.0 | 4.2 | 3.3 | 0.1 | 0.0 | 0.5 | 0.0 | 0.0 | 0.0 | 0.0 | 0.0 |
| 5 | 66.9 | 3.9 | 8.6 | 19.0 | 2.1 | 18.0 | 1.7 | 0.0 | 0.0 | 0.0 | 0.3 | 0.0 |
| 6 | 81.0 | 17.4 | 11.9 | 2.8 | 1.1 | 1.6 | 0.5 | 0.0 | 0.0 | 0.0 | 0.0 | 0.0 |
| 7 | 42.6 | 20.3 | 17.6 | 5.7 | 0.4 | 10.0 | 0.0 | 0.0 | 0.0 | 0.0 | 0.3 | 0.0 |
| 8 | 2.8 | 9.6 | 1.9 | 1.4 | 0.5 | 4.4 | 0.8 | 0.0 | 0.0 | 0.0 | 0.5 | 0.0 |
| 9 | 3.1 | 1.0 | 1.5 | 3.8 | 1.1 | 12.5 | 0.2 | 3.1 | 0.0 | 0.0 | 1.9 | 0.0 |

77

78 **Table S5. The distribution of particulate I/SVOCs (mg km⁻¹) at high-speed stage for non-(DPF + DOC) vehicles**
 79 **separated by volatility bins and the O:C ratio.**

| log ₁₀ C * (μg m ⁻³) | O:C ratio | | | | | | | | | | | |
|---|-----------|-------------|-------------|-------------|-------------|-------------|-------------|-------------|-------------|-------------|-------------|-------------|
| | 0- 0.1 | 0.1- 0.2 | 0.2- 0.3 | 0.3- 0.4 | 0.4- 0.5 | 0.5- 0.6 | 0.6- 0.7 | 0.7- 0.8 | 0.8- 0.9 | 0.9- 1.0 | 1.0- 1.1 | 1.1- 1.2 |
| -4 | 0.0 | 0.0 | 0.0 | 0.0 | 0.0 | 0.0 | 0.0 | 0.0 | 0.0 | 0.0 | 0.0 | 0.0 |
| -3 | 0.3 | 0.1 | 0.1 | 0.0 | 0.0 | 0.0 | 0.0 | 0.0 | 0.0 | 0.0 | 0.0 | 0.0 |
| -2 | 0.3 | 0.1 | 0.0 | 0.0 | 0.0 | 0.0 | 0.0 | 0.0 | 0.0 | 0.0 | 2.4 | 0.0 |
| -1 | 0.6 | 0.0 | 0.1 | 0.0 | 0.0 | 0.0 | 0.0 | 0.0 | 0.0 | 0.0 | 0.0 | 0.0 |
| 0 | 3.1 | 0.3 | 0.0 | 0.0 | 0.0 | 0.0 | 0.0 | 0.0 | 0.0 | 0.0 | 3.7 | 0.0 |
| 1 | 2.6 | 2.1 | 0.4 | 0.0 | 0.0 | 0.0 | 0.0 | 0.0 | 0.0 | 0.0 | 0.0 | 0.0 |
| 2 | 10.1 | 1.4 | 4.4 | 0.1 | 0.0 | 0.0 | 0.0 | 0.0 | 0.0 | 0.0 | 0.0 | 0.0 |
| 3 | 45.5 | 3.7 | 1.1 | 0.2 | 0.0 | 0.1 | 0.0 | 0.0 | 0.0 | 0.0 | 0.0 | 0.0 |
| 4 | 37.4 | 2.0 | 2.3 | 1.4 | 0.2 | 0.1 | 0.0 | 0.0 | 0.0 | 0.0 | 0.0 | 0.0 |
| 5 | 8.3 | 1.5 | 4.1 | 5.3 | 0.9 | 17.0 | 0.7 | 0.0 | 0.0 | 0.0 | 0.0 | 0.0 |
| 6 | 17.7 | 8.4 | 6.2 | 1.9 | 0.3 | 0.0 | 0.0 | 0.0 | 0.0 | 0.0 | 0.0 | 0.0 |
| 7 | 21.1 | 11.7 | 5.1 | 4.0 | 0.0 | 11.3 | 0.1 | 0.0 | 0.0 | 0.0 | 0.0 | 0.0 |
| 8 | 2.0 | 5.7 | 0.2 | 0.2 | 0.3 | 1.2 | 0.7 | 0.0 | 0.0 | 0.0 | 0.4 | 0.0 |
| 9 | 7.1 | 0.8 | 0.5 | 4.0 | 0.6 | 8.5 | 0.2 | 7.5 | 0.0 | 0.0 | 0.4 | 0.0 |

80

81 **Table S6. The distribution of particulate I/SVOCs (mg km^{-1}) at whole driving cycle (W_cold) for non-(DPF + DOC)**
 82 **vehicles separated by volatility bins and the O:C ratio.**

| $\log_{10}C$ * ($\mu\text{g m}^{-3}$) | O:C ratio | | | | | | | | | | | |
|--|-----------|---------|---------|---------|---------|---------|---------|---------|---------|---------|---------|---------|
| | 0-0.1 | 0.1-0.2 | 0.2-0.3 | 0.3-0.4 | 0.4-0.5 | 0.5-0.6 | 0.6-0.7 | 0.7-0.8 | 0.8-0.9 | 0.9-1.0 | 1.0-1.1 | 1.1-1.2 |
| -4 | 121.0 | 56.7 | 61.6 | 21.6 | 9.6 | 7.0 | 3.7 | 1.7 | 0.1 | 0.0 | 3.2 | 0.3 |
| -3 | 162.3 | 88.8 | 63.1 | 35.8 | 13.0 | 9.0 | 6.7 | 2.2 | 1.2 | 0.0 | 1.0 | 0.6 |
| -2 | 18.7 | 9.0 | 7.5 | 3.6 | 1.5 | 1.2 | 0.7 | 0.3 | 0.3 | 0.0 | 1.3 | 0.0 |
| -1 | 6.7 | 1.4 | 1.4 | 0.5 | 0.4 | 0.3 | 0.0 | 0.1 | 0.0 | 0.0 | 0.0 | 0.0 |
| 0 | 5.6 | 0.9 | 0.2 | 0.0 | 0.0 | 0.0 | 0.0 | 0.0 | 0.0 | 0.0 | 2.5 | 0.0 |
| 1 | 16.9 | 1.7 | 1.0 | 0.2 | 0.0 | 0.0 | 0.0 | 0.0 | 0.0 | 0.0 | 0.6 | 0.0 |
| 2 | 21.4 | 3.4 | 7.1 | 0.2 | 0.0 | 0.0 | 0.0 | 0.1 | 0.0 | 0.0 | 0.0 | 0.0 |
| 3 | 84.2 | 10.2 | 1.4 | 0.5 | 0.1 | 0.2 | 0.0 | 0.0 | 0.0 | 0.0 | 0.0 | 0.0 |
| 4 | 106.0 | 3.8 | 4.4 | 3.0 | 0.2 | 0.1 | 0.3 | 0.0 | 0.0 | 0.0 | 0.0 | 0.0 |
| 5 | 38.3 | 3.3 | 8.5 | 14.3 | 2.2 | 22.6 | 1.6 | 0.1 | 0.0 | 0.0 | 0.1 | 0.0 |
| 6 | 61.3 | 18.1 | 12.1 | 3.1 | 1.5 | 1.2 | 0.2 | 0.0 | 0.0 | 0.0 | 0.0 | 0.0 |
| 7 | 55.8 | 35.5 | 17.2 | 10.3 | 1.3 | 14.9 | 0.0 | 0.0 | 0.0 | 0.0 | 0.1 | 0.0 |
| 8 | 4.8 | 11.9 | 1.3 | 1.0 | 1.3 | 4.0 | 1.7 | 0.4 | 0.0 | 0.0 | 0.7 | 0.0 |
| 9 | 27.4 | 2.3 | 1.1 | 6.7 | 1.2 | 17.5 | 1.4 | 5.1 | 0.0 | 0.0 | 1.6 | 0.0 |

83

84 **Table S7. The distribution of particulate I/SVOCs (mg km^{-1}) at whole driving cycle (W_hot) for non-(DPF + DOC)**
 85 **vehicles separated by volatility bins and the O:C ratio.**

| $\log_{10}C$ * ($\mu\text{g m}^{-3}$) | O:C ratio | | | | | | | | | | | |
|--|-----------|---------|---------|---------|---------|---------|---------|---------|---------|---------|---------|---------|
| | 0-0.1 | 0.1-0.2 | 0.2-0.3 | 0.3-0.4 | 0.4-0.5 | 0.5-0.6 | 0.6-0.7 | 0.7-0.8 | 0.8-0.9 | 0.9-1.0 | 1.0-1.1 | 1.1-1.2 |
| -4 | 12.0 4 | 0.00 | 0.42 | 0.00 | 0.00 | 0.00 | 0.00 | 0.00 | 0.00 | 0.00 | 0.00 | 0.00 |
| -3 | 25.5 8 | 1.02 | 0.00 | 0.00 | 0.15 | 0.26 | 0.00 | 0.00 | 0.00 | 0.00 | 0.00 | 0.00 |
| -2 | 11.3 8 | 0.00 | 0.00 | 0.00 | 0.00 | 0.00 | 0.19 | 0.00 | 0.00 | 0.00 | 0.00 | 0.00 |
| -1 | 3.84 | 0.12 | 0.06 | 0.00 | 0.00 | 0.00 | 0.00 | 0.00 | 0.00 | 0.00 | 0.00 | 0.00 |
| 0 | 2.91 | 0.73 | 0.02 | 0.00 | 0.00 | 0.07 | 0.02 | 0.00 | 0.00 | 0.00 | 0.00 | 0.00 |
| 1 | 2.15 | 0.78 | 0.13 | 0.02 | 0.00 | 0.05 | 0.00 | 0.00 | 0.00 | 0.00 | 0.00 | 0.00 |
| 2 | 8.52 | 2.37 | 4.35 | 0.33 | 0.00 | 0.00 | 0.11 | 0.00 | 0.00 | 0.00 | 0.00 | 0.00 |
| 3 | 17.0 1 | 3.75 | 0.30 | 0.43 | 0.08 | 0.05 | 0.00 | 0.00 | 0.00 | 0.00 | 0.00 | 0.00 |
| 4 | 6.99 | 1.66 | 1.78 | 1.10 | 0.09 | 0.01 | 0.00 | 0.00 | 0.00 | 0.00 | 0.00 | 0.00 |
| 5 | 4.09 | 6.93 | 8.11 | 1.24 | 1.49 | 5.54 | 0.86 | 0.00 | 0.00 | 0.00 | 0.02 | 0.00 |
| 6 | 12.1 3 | 5.50 | 8.94 | 1.02 | 1.26 | 0.49 | 0.00 | 0.00 | 0.00 | 0.00 | 0.00 | 0.00 |
| 7 | 8.92 | 4.75 | 1.17 | 2.45 | 0.21 | 1.60 | 0.19 | 0.00 | 0.00 | 0.00 | 0.00 | 0.00 |
| 8 | 0.30 | 3.21 | 0.09 | 0.00 | 0.31 | 0.00 | 0.82 | 0.00 | 0.00 | 0.00 | 0.00 | 0.00 |
| 9 | 0.81 | 1.44 | 0.17 | 1.41 | 1.27 | 2.23 | 0.54 | 0.00 | 0.00 | 0.00 | 0.29 | 0.00 |

86

87 **Table S8. The distribution of particulate I/SVOCs (mg km⁻¹) at low-speed stage for (DPF + DOC) vehicles separated**
 88 **by volatility bins and the O:C ratio.**

| log ₁₀ C * (μg m ⁻³) | O:C ratio | | | | | | | | | | | |
|---|------------|-------------|-------------|-------------|-------------|-------------|-------------|-------------|-------------|-------------|-------------|-------------|
| | 0-0.1 | 0.1- 0.2 | 0.2- 0.3 | 0.3- 0.4 | 0.4- 0.5 | 0.5- 0.6 | 0.6- 0.7 | 0.7- 0.8 | 0.8- 0.9 | 0.9- 1.0 | 1.0- 1.1 | 1.1- 1.2 |
| -4 | 3.0 | 0.0 | 1.5 | 0.9 | 0.0 | 11.1 | 0.0 | 0.7 | 0.0 | 0.0 | 0.0 | 0.0 |
| -3 | 9.2 | 2.5 | 2.8 | 2.2 | 0.5 | 0.0 | 0.3 | 0.0 | 0.0 | 0.0 | 0.0 | 0.0 |
| -2 | 25.7 | 0.7 | 0.3 | 0.3 | 0.3 | 0.0 | 0.0 | 1.2 | 0.0 | 0.0 | 0.2 | 0.0 |
| -1 | 27.8 | 4.8 | 0.7 | 1.0 | 0.3 | 0.0 | 0.0 | 0.0 | 0.1 | 0.0 | 0.0 | 0.0 |
| 0 | 83.8 | 6.9 | 3.0 | 0.4 | 0.1 | 2.1 | 1.0 | 0.2 | 0.0 | 0.0 | 0.5 | 0.0 |
| 1 | 46.9 | 29.1 | 9.5 | 7.6 | 3.0 | 1.3 | 1.2 | 0.2 | 0.2 | 0.0 | 0.2 | 0.0 |
| 2 | 99.2 | 35.2 | 115.4 | 3.5 | 1.3 | 0.2 | 2.7 | 0.7 | 0.1 | 0.0 | 8.4 | 0.0 |
| 3 | 328.0 | 48.3 | 10.0 | 5.3 | 0.7 | 7.8 | 0.3 | 0.3 | 0.0 | 0.0 | 0.2 | 0.0 |
| 4 | 132.2 | 10.8 | 41.6 | 49.6 | 2.0 | 0.3 | 0.4 | 0.0 | 0.0 | 0.0 | 0.2 | 0.0 |
| 5 | 87.7 | 12.2 | 49.9 | 108.9 | 17.2 | 115.5 | 4.1 | 0.3 | 0.0 | 0.0 | 0.4 | 0.0 |
| 6 | 408.6 | 237.5 | 74.7 | 32.8 | 17.8 | 5.2 | 2.2 | 0.0 | 0.0 | 0.0 | 0.0 | 0.0 |
| 7 | 1365. 3 | 662.0 | 222.4 | 57.6 | 6.3 | 132.4 | 4.4 | 1.5 | 0.0 | 0.0 | 1.8 | 0.0 |
| 8 | 77.8 | 302.8 | 3.4 | 1.2 | 9.7 | 52.1 | 4.9 | 0.8 | 0.0 | 0.0 | 1.8 | 0.0 |
| 9 | 294.2 | 26.2 | 33.5 | 91.2 | 18.9 | 216.5 | 29.2 | 0.0 | 0.0 | 0.0 | 34.8 | 0.0 |

89

90 **Table S9. The distribution of particulate I/SVOCs (mg km^{-1}) at middle-speed stage for (DPF + DOC) vehicles separated**
 91 **by volatility bins and the O:C ratio.**

| $\log_{10}C$ * ($\mu\text{g m}^{-3}$) | O:C ratio | | | | | | | | | | | |
|--|-----------|---------|---------|---------|---------|---------|---------|---------|---------|---------|---------|---------|
| | 0-0.1 | 0.1-0.2 | 0.2-0.3 | 0.3-0.4 | 0.4-0.5 | 0.5-0.6 | 0.6-0.7 | 0.7-0.8 | 0.8-0.9 | 0.9-1.0 | 1.0-1.1 | 1.1-1.2 |
| -4 | 1.2 | 0.9 | 0.6 | 0.6 | 0.0 | 2.4 | 0.0 | 0.0 | 0.0 | 0.0 | 0.0 | 0.0 |
| -3 | 1.4 | 0.4 | 0.2 | 0.2 | 0.1 | 3.6 | 0.0 | 0.0 | 0.0 | 0.0 | 0.0 | 0.0 |
| -2 | 1.2 | 0.1 | 0.0 | 0.0 | 0.0 | 4.1 | 0.0 | 0.0 | 0.0 | 0.0 | 0.0 | 0.0 |
| -1 | 1.3 | 0.1 | 0.0 | 0.1 | 0.0 | 0.1 | 0.0 | 0.0 | 0.0 | 0.0 | 1.7 | 0.0 |
| 0 | 13.4 | 0.4 | 0.4 | 0.1 | 0.2 | 0.0 | 0.3 | 0.0 | 0.0 | 0.0 | 0.3 | 0.0 |
| 1 | 3.5 | 4.8 | 1.0 | 0.2 | 0.0 | 0.1 | 0.0 | 0.0 | 0.0 | 0.0 | 1.0 | 0.0 |
| 2 | 10.7 | 3.2 | 5.6 | 0.3 | 0.0 | 0.0 | 0.0 | 0.0 | 0.0 | 0.0 | 0.0 | 0.0 |
| 3 | 12.4 | 5.6 | 0.7 | 0.6 | 0.0 | 0.4 | 0.0 | 0.0 | 0.0 | 0.0 | 0.0 | 0.0 |
| 4 | 6.0 | 0.8 | 2.9 | 8.5 | 0.1 | 0.0 | 0.0 | 0.0 | 0.0 | 0.0 | 0.0 | 0.0 |
| 5 | 5.1 | 2.2 | 7.9 | 9.9 | 2.2 | 15.6 | 1.8 | 0.0 | 0.1 | 0.0 | 0.0 | 0.0 |
| 6 | 21.4 | 18.6 | 11.5 | 3.5 | 2.8 | 1.3 | 0.8 | 0.1 | 0.0 | 0.0 | 0.1 | 0.0 |
| 7 | 39.3 | 28.2 | 24.9 | 6.2 | 0.7 | 7.5 | 0.4 | 0.0 | 0.0 | 0.0 | 0.0 | 0.0 |
| 8 | 8.7 | 14.5 | 3.5 | 1.0 | 1.9 | 3.7 | 1.3 | 0.0 | 0.0 | 0.0 | 0.1 | 0.0 |
| 9 | 11.7 | 3.4 | 2.2 | 3.8 | 0.7 | 14.1 | 1.5 | 0.5 | 0.0 | 0.0 | 1.7 | 0.0 |

92

93 **Table S10. The distribution of particulate I/SVOCs (mg km^{-1}) at high-speed stage for (DPF + DOC) vehicles separated**
 94 **by volatility bins and the O:C ratio.**

| $\log_{10}C$ * ($\mu\text{g m}^{-3}$) | O:C ratio | | | | | | | | | | | |
|--|-----------|---------|---------|---------|---------|---------|---------|---------|---------|---------|---------|---------|
| | 0-0.1 | 0.1-0.2 | 0.2-0.3 | 0.3-0.4 | 0.4-0.5 | 0.5-0.6 | 0.6-0.7 | 0.7-0.8 | 0.8-0.9 | 0.9-1.0 | 1.0-1.1 | 1.1-1.2 |
| -4 | 1.6 | 0.4 | 0.1 | 0.3 | 0.0 | 5.2 | 0.0 | 0.0 | 0.0 | 0.0 | 0.0 | 0.0 |
| -3 | 1.0 | 0.3 | 0.3 | 0.2 | 0.0 | 3.9 | 0.0 | 0.0 | 0.0 | 0.0 | 0.0 | 0.0 |
| -2 | 1.0 | 0.0 | 0.1 | 0.0 | 0.0 | 0.5 | 0.0 | 0.0 | 0.0 | 0.0 | 0.0 | 0.0 |
| -1 | 1.1 | 0.0 | 0.0 | 0.1 | 0.0 | 0.1 | 0.0 | 0.0 | 0.0 | 0.0 | 0.0 | 0.0 |
| 0 | 3.7 | 0.3 | 0.1 | 0.1 | 0.0 | 0.1 | 0.1 | 0.0 | 0.0 | 0.0 | 4.0 | 0.0 |
| 1 | 1.6 | 2.4 | 0.4 | 0.2 | 0.0 | 0.1 | 0.0 | 0.0 | 0.0 | 0.0 | 0.5 | 0.0 |
| 2 | 7.5 | 3.3 | 11.8 | 0.5 | 0.0 | 0.0 | 0.1 | 0.0 | 0.0 | 0.0 | 1.4 | 0.0 |
| 3 | 17.2 | 3.6 | 0.7 | 0.4 | 0.1 | 0.1 | 0.0 | 0.0 | 0.0 | 0.0 | 0.0 | 0.0 |
| 4 | 6.0 | 0.7 | 2.3 | 8.3 | 0.0 | 0.1 | 0.0 | 0.0 | 0.0 | 0.0 | 0.0 | 0.0 |
| 5 | 5.9 | 1.1 | 5.0 | 16.0 | 1.5 | 20.9 | 2.2 | 0.0 | 0.0 | 0.0 | 0.1 | 0.0 |
| 6 | 19.5 | 18.0 | 11.2 | 3.3 | 3.8 | 1.4 | 0.8 | 0.0 | 0.0 | 0.0 | 0.1 | 0.0 |
| 7 | 56.9 | 45.6 | 29.1 | 4.9 | 0.3 | 15.6 | 0.7 | 0.5 | 0.0 | 0.0 | 0.3 | 0.2 |
| 8 | 4.0 | 11.2 | 1.2 | 0.6 | 0.8 | 1.9 | 1.5 | 0.1 | 0.0 | 0.0 | 0.3 | 0.0 |
| 9 | 7.3 | 1.9 | 2.7 | 6.0 | 1.2 | 8.9 | 2.9 | 0.3 | 0.0 | 0.0 | 5.6 | 0.0 |

95

96
97

Table S11. The distribution of particulate I/SVOCs (mg km^{-1}) at whole driving cycle (W_cold) for (DPF + DOC) vehicles separated by volatility bins and the O:C ratio.

| log ₁₀ C * ($\mu\text{g m}^{-3}$) | O:C ratio | | | | | | | | | | | |
|---|-----------|---------|---------|---------|---------|---------|---------|---------|---------|---------|---------|---------|
| | 0-0.1 | 0.1-0.2 | 0.2-0.3 | 0.3-0.4 | 0.4-0.5 | 0.5-0.6 | 0.6-0.7 | 0.7-0.8 | 0.8-0.9 | 0.9-1.0 | 1.0-1.1 | 1.1-1.2 |
| -4 | 1.5 | 0.6 | 0.4 | 0.5 | 0.0 | 4.0 | 0.0 | 0.0 | 0.0 | 0.0 | 0.0 | 0.0 |
| -3 | 1.4 | 0.4 | 0.3 | 0.2 | 0.0 | 3.6 | 0.0 | 0.0 | 0.0 | 0.0 | 0.0 | 0.0 |
| -2 | 1.8 | 0.1 | 0.0 | 0.0 | 0.0 | 2.2 | 0.0 | 0.0 | 0.0 | 0.0 | 0.0 | 0.0 |
| -1 | 1.9 | 0.2 | 0.0 | 0.2 | 0.0 | 0.1 | 0.0 | 0.0 | 0.0 | 0.0 | 0.8 | 0.0 |
| 0 | 10.7 | 0.6 | 0.3 | 0.1 | 0.1 | 0.1 | 0.2 | 0.0 | 0.0 | 0.0 | 2.1 | 0.0 |
| 1 | 3.8 | 4.3 | 0.9 | 0.4 | 0.1 | 0.1 | 0.1 | 0.0 | 0.0 | 0.0 | 0.8 | 0.0 |
| 2 | 11.7 | 4.2 | 11.6 | 0.5 | 0.1 | 0.0 | 0.1 | 0.0 | 0.0 | 0.0 | 0.9 | 0.0 |
| 3 | 23.5 | 5.8 | 1.0 | 0.6 | 0.1 | 0.5 | 0.0 | 0.0 | 0.0 | 0.0 | 0.0 | 0.0 |
| 4 | 9.5 | 1.0 | 3.7 | 9.5 | 0.1 | 0.0 | 0.0 | 0.0 | 0.0 | 0.0 | 0.0 | 0.0 |
| 5 | 7.8 | 1.9 | 7.7 | 15.6 | 2.3 | 20.9 | 2.0 | 0.0 | 0.0 | 0.0 | 0.1 | 0.0 |
| 6 | 31.3 | 24.4 | 13.1 | 4.2 | 3.7 | 1.5 | 0.8 | 0.1 | 0.0 | 0.0 | 0.1 | 0.0 |
| 7 | 84.7 | 54.2 | 32.4 | 7.0 | 0.6 | 14.9 | 0.6 | 0.3 | 0.0 | 0.0 | 0.2 | 0.1 |
| 8 | 8.4 | 20.9 | 2.4 | 0.8 | 1.6 | 4.2 | 1.5 | 0.1 | 0.0 | 0.0 | 0.2 | 0.0 |
| 9 | 17.5 | 3.3 | 3.3 | 7.3 | 1.5 | 17.3 | 3.0 | 0.4 | 0.0 | 0.0 | 4.5 | 0.0 |

98

99
100

Table S12. The distribution of particulate I/SVOCs (mg km^{-1}) at whole driving cycle (W_hot) for (DPF + DOC) vehicles separated by volatility bins and the O:C ratio.

| $\log_{10}C$ * ($\mu\text{g m}^{-3}$) | O:C ratio | | | | | | | | | | | |
|--|-----------|---------|---------|---------|---------|---------|---------|---------|---------|---------|---------|---------|
| | 0-0.1 | 0.1-0.2 | 0.2-0.3 | 0.3-0.4 | 0.4-0.5 | 0.5-0.6 | 0.6-0.7 | 0.7-0.8 | 0.8-0.9 | 0.9-1.0 | 1.0-1.1 | 1.1-1.2 |
| -4 | 0.21 | 0.26 | 0.10 | 0.05 | 0.00 | 5.27 | 0.00 | 0.00 | 0.00 | 0.00 | 0.00 | 0.00 |
| -3 | 0.38 | 0.09 | 0.06 | 0.00 | 0.02 | 1.74 | 0.00 | 0.07 | 0.01 | 0.00 | 0.00 | 0.00 |
| -2 | 0.38 | 0.03 | 0.02 | 0.00 | 0.00 | 0.29 | 0.00 | 0.00 | 0.00 | 0.00 | 0.00 | 0.00 |
| -1 | 0.43 | 0.06 | 0.01 | 0.04 | 0.00 | 0.04 | 0.00 | 0.00 | 0.00 | 0.00 | 5.44 | 0.00 |
| 0 | 2.34 | 0.31 | 0.11 | 0.03 | 0.00 | 0.00 | 0.00 | 0.00 | 0.00 | 0.00 | 1.13 | 0.00 |
| 1 | 1.47 | 0.88 | 0.10 | 0.08 | 0.01 | 0.03 | 0.00 | 0.01 | 0.01 | 0.00 | 0.74 | 0.00 |
| 2 | 7.49 | 2.15 | 6.00 | 0.15 | 0.04 | 0.01 | 0.05 | 0.00 | 0.01 | 0.00 | 0.36 | 0.00 |
| 3 | 7.83 | 6.48 | 0.51 | 0.52 | 0.07 | 0.19 | 0.01 | 0.00 | 0.00 | 0.00 | 0.00 | 0.00 |
| 4 | 3.58 | 0.48 | 1.93 | 3.60 | 0.06 | 0.03 | 0.00 | 0.00 | 0.00 | 0.00 | 0.01 | 0.00 |
| 5 | 7.51 | 1.62 | 5.82 | 2.40 | 2.23 | 16.47 | 1.09 | 0.12 | 0.00 | 0.00 | 0.78 | 0.00 |
| 6 | 22.2 1 | 12.66 | 7.23 | 9.99 | 2.40 | 2.96 | 1.32 | 0.08 | 0.00 | 0.00 | 0.21 | 0.00 |
| 7 | 31.7 0 | 12.19 | 8.89 | 6.74 | 0.05 | 5.74 | 0.25 | 0.00 | 0.09 | 0.00 | 0.11 | 0.00 |
| 8 | 7.02 | 5.74 | 7.26 | 0.27 | 0.83 | 5.43 | 2.50 | 0.53 | 0.00 | 0.00 | 0.15 | 0.00 |
| 9 | 5.58 | 2.20 | 2.39 | 3.19 | 0.20 | 5.53 | 1.06 | 0.10 | 0.00 | 0.00 | 4.43 | 0.00 |

101

102 **References:**

- 103 <https://www.epa.gov/tsca-screening-tools/download-epi-suite-estimation-program-interface-v411>. (2021,
104 March 12, 2021). EPI Suite™ - Estimation Program Interface v4.11. Retrieved from
105 <https://www.epa.gov/tsca-screening-tools/download-epi-suite-estimation-program-interface-v411>
- 106 May, A. A., Presto, A. A., Hennigan, C. J., Nguyen, N. T., Gordon, T. D., & Robinson, A. L. (2013a). Gas-particle
107 partitioning of primary organic aerosol emissions: (1) Gasoline vehicle exhaust. *Atmospheric*
108 *Environment*, 77, 128-139. doi:10.1016/j.atmosenv.2013.04.060
- 109 May, A. A., Presto, A. A., Hennigan, C. J., Nguyen, N. T., Gordon, T. D., & Robinson, A. L. (2013b). Gas-Particle
110 Partitioning of Primary Organic Aerosol Emissions: (2) Diesel Vehicles. *Environmental Science &*
111 *Technology*, 47(15), 8288-8296. doi:10.1021/es400782j
- 112 Zhao, Y., Nguyen, N. T., Presto, A. A., Hennigan, C. J., May, A. A., & Robinson, A. L. (2015). Intermediate
113 Volatility Organic Compound Emissions from On-Road Diesel Vehicles: Chemical Composition,
114 Emission Factors, and Estimated Secondary Organic Aerosol Production. *Environmental Science and*
115 *Technology*, 49(19), 11516-11526. doi:10.1021/acs.est.5b02841